

Analysis of side-plated reinforced concrete beams with partial interaction

W.H. Siu and R.K.L. Su*

Department of Civil Engineering, The University of Hong Kong, Pokfulam Road, Hong Kong, PRC

(Received June, 26, 2009, Accepted August 4, 2009)

Abstract. Existing reinforced concrete (RC) beams can be strengthened with externally bolted steel plates to the sides of beams. The effectiveness of this type of bolted side-plate (BSP) beam can however be affected by partial interaction between the steel plates and RC beams due to the mechanical slip of bolts. To avoid over-estimation of the flexural strength and ensure accurate prediction of the load-deformation response of the beams, the effect of partial interaction has to be properly considered. In this paper, a special non-linear macro-finite-element model that takes into account the effects of partial interaction is proposed. The RC beam and the steel plates are modelled as two different elements, interacting through discrete groups of bolts. A layered method is adopted for the formulation of the RC beam and steel plate elements, while a special non-linear model based on a kinematic hardening assumption for the bolts is used to simulate the bolt group effect. The computer program SiBAN was developed based on the proposed approach. Comparison with the available experimental results shows that SiBAN can accurately predict the partial interaction behaviour of the BSP beams. Further numerical simulations show that the interaction between the RC beam and the steel plates is greatly reduced by the formation of plastic hinges and should be considered in analyses of the strengthened beams.

Keywords: partial interaction; strengthening; reinforced concrete; plate; finite element; slip.

1. Introduction

Due to the deterioration of materials and the demand for additional strength, existing beam structures often need retrofitting. One of the common ways to strengthen existing reinforced concrete (RC) beams is to anchor steel plates to the side faces of the beams with bolts (herein referred to as bolted side-plated (BSP) beams), which generally enhances both the flexural and shear performance of the beams.

The behaviour of BSP beams is different from those retrofitted with adhesive-bonded steel plates. In BSP beams, due to the use of bolts, the plates will slip relative to the RC beam under loading in both longitudinal and transverse directions so that the bolts can deform and resist the shear flow between the RC beam and the steel plates. Such difference in deformation is known as partial interaction (Oehlers *et al.* 1997) and it reduces the strain of steel plates at the critical section at ultimate state, leading to the un-yielded situation in steel plate and eventually the flexural strength reduction in BSP beams. Such strength reduction can be more than 20% of additional strength provided by the strengthening plates (Ahmed *et al.* 2000, Oehlers *et al.* 2000), which is significant and can lead to failure of the strengthened beam if it is not properly considered.

* Corresponding author, Assistant Professor, E-mail: klsu@hkucc.hku.hk

The problem of partial interaction is classic in standard composite beams where concrete slab is interacted with steel beams with the use of shear studs. Many researches had been carried out to simulate the non-linear response of composite beams with presence of partial interaction (Arizumi and Hamada 1981, Ayoub 2000, Dall'Asta and Zona 2004, Daniels and Crisinel 1993, Faella *et al.* 2002, Gattesco 1999, Johnson and Molenstra 1991, Ranzi *et al.* 2004, Yam and Chapman 1968, Johnson and Molenstra 1991). Different numerical methods like non-linear finite element analysis based on displacement field formulation (Arizumi and Hamada 1981, Daniels and Crisinel 1993, Gattesco 1999), displacement and force fields formulations (Ayoub 2000), 'direct' analysis based on exact solution of slip (Faella *et al.* 2002, Ranzi *et al.* 2004) and finite difference methods (Yam and Chapman 1968, Johnson and Molenstra 1991) were used. These approaches, though different, are conceptually similar as they all attempted to incorporate partial interaction into analysis by defining separate nodes to the concrete slab and the steel beams, hence allowing relative movements between the two components.

The extensive use of numerical methods to handle to problem of partial interaction highlighted complexity of partial interaction in composite beam systems. Yet, these approaches, as developed for standard composite beams, cannot be used directly to model the response of BSP beams. Different from standard composite beam, where the partial interaction is dominant in longitudinal direction, the partial interaction in BSP beams occur in both longitudinal and transverse directions. This means that the mechanical connectors are subjected to both longitudinal and transverse shear simultaneously. To simulate the response of BSP beams, an analysis capable of modelling the non-linear interaction of longitudinal and transverse interactions of shear connectors is necessary.

In this paper, a non-linear macro-finite-element method that takes into account the interactions of longitudinal and transverse partial interactions is proposed. Reinforced concrete beams and steel plates are modelled as two different elements that interact with each other through discrete groups of bolts. The formulation of the element stiffness matrix is based on a layered finite element model commonly used to consider material non-linearity in RC structures. To account for the inelastic behaviour of bolt groups subject to longitudinal and transverse shear, a non-linear model of bolts under multi-directional shear together with a procedure to formulate the non-linear tangential stiffness matrix of bolt groups is adopted.

Using the proposed theory, a computer program SiBAN is developed. Numerical simulations were carried out to illustrate slip responses in the longitudinal and transverse directions along with a new type of partial interaction (the rotational partial interaction) for BSP beams. The rotational partial interaction is significant for the load distribution in connectors when more than one row of connectors is used. The pre-peak responses of the load-deformation of beams and the partial interactions are investigated in detail. As the present side-plate strengthening system is likely to be governed by gravity loads, a system collapse would take place when the applied load exceeds the load-carrying capacity. Consequently, the present numerical study focuses on pre-peak behaviour, and a simple load-controlled solution procedure is adopted to solve the non-linear equations.

2. Formulation of non-linear model for bolt connections

2.1 General

Consider a BSP beam as shown in Fig. 1(a) with a steel plate anchored by $n + 1$ bolt groups. The

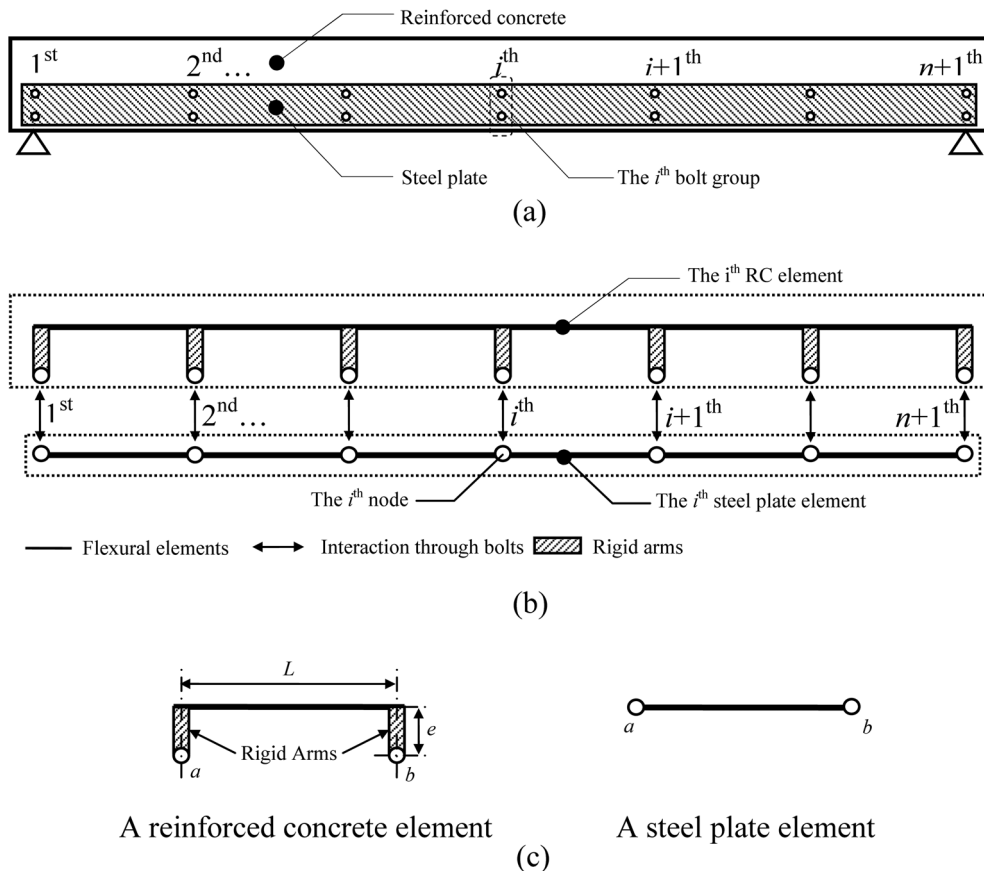


Fig. 1 Structural model of a BSP beam (a) prototype, (b) structural model and (c) typical RC & steel plate elements

stiffness centroids of the bolt groups are located at the geometric centroids of the steel plates.

The corresponding idealized structural model of the strengthened beam is shown in Fig. 1(b). Nodes, defined at the centroids of the bolt groups, are numbered from left to right. The whole beam is discretized into n pairs of RC beam and steel plate non-linear macro-finite-elements. The length of the i^{th} element is equal to the separation between the i^{th} and the $i+1^{\text{th}}$ bolt groups. The formulation of the stiffness matrices of the elements is provided in the next section. Since the centroidal axis of the RC beam is located above the centroid of the steel plates, rigid arms are added at the ends of the RC beam elements so that they can interact with each other through the dimensionless bolt groups. Typical RC beam and steel plate elements are shown in Fig. 1(c). The nodes on the left and right sides of the RC beam and steel plate elements are named Node a and Node b respectively. This means that the i^{th} bolt group is connected to Node b of the $i-1^{\text{th}}$ RC beam and steel plate elements together with Node a of the i^{th} RC beam and steel plate elements. To account for the effects of partial interactions in the analysis, we adopted non-linear bolt groups with finite stiffness, the details of which will be described in Section 2.3.

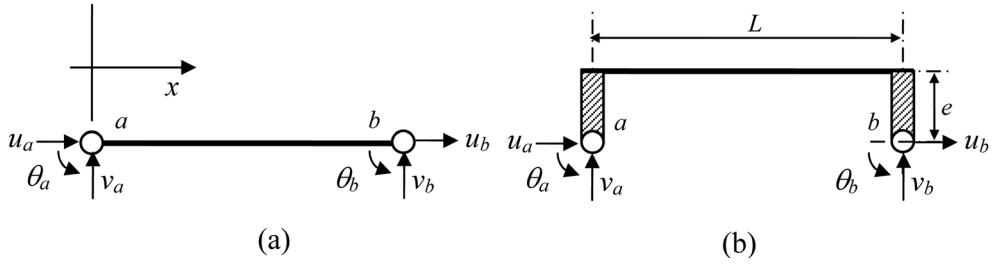


Fig. 2 Sign conventions for (a) a flexural element and (b) a concrete element

2.2 Formulation of the RC beam and steel plate elements

The longitudinal and vertical displacement shape functions corresponding to unit nodal displacements $(u_a, u_b, v_a, v_b, \theta_a, \theta_b)$ of a flexural element (Fig. 2(a)) are assumed to be

$$u(x) = [(1-\xi), \xi, 0, 0, 0, 0] \quad (1)$$

$$v(x) = [0, 0, (1-3\xi^2+2\xi^3), (3\xi^2-2\xi^3), L(\xi-2\xi^2+\xi^3), L(-\xi^2+\xi^3)] \quad (2)$$

where $\xi = x/L$ is the natural coordinate. The strain at any point within the member can be divided into an axial component and a bending component

$$\varepsilon(x, y) = \varepsilon_{axial}(x, y) + \varepsilon_{bending}(x, y) \quad (3)$$

Assuming the axial strain is evenly distributed along the element and across the section, we have

$$\varepsilon_{axial}(x, y) = \frac{u_b - u_a}{L} = \left[-\frac{1}{L}, \frac{1}{L} \right] \times [u_a, u_b]^T \quad (4)$$

Applying the hypothesis that plane sections remain plane after bending, the bending strain $\varepsilon_{bending}(x, y)$ can be expressed in terms of the curvature $\phi(x)$ of the section

$$\varepsilon_{bending}(x, y) = \phi(x)y \quad (5)$$

Invoking the relationship $\phi(x) = v''(x)$ and differentiating Eq. (2) twice with respect to x , Eq. (5) becomes

$$\varepsilon_{bending}(x, y) = \left[\frac{6}{L^2}y(1-2\xi), \frac{6}{L^2}y(-1+2\xi), \frac{2}{L}y(2-3\xi), \frac{2}{L}y(1-3\xi) \right] \quad (6)$$

Combining Eqs. (4) and (6), the strain-displacement matrix \mathbf{B} at any point (x, y) is

$$\mathbf{B} = \left[-\frac{1}{L}, \frac{1}{L}, \frac{6}{L^2}y(-1+2\xi), \frac{6}{L^2}y(1-2\xi), \frac{2}{L}y(2-3\xi), \frac{2}{L}y(1-3\xi) \right] \quad (7)$$

Eq. (7) can be decomposed into the corresponding axial component \mathbf{B}_a and bending component $y\mathbf{B}_b$, i.e.

$$\mathbf{B} = [\mathbf{B}_a, y\mathbf{B}_b] \quad (8)$$

where $\mathbf{B}_a = \left[\frac{-1}{L}, \frac{1}{L} \right]$, $\mathbf{B}_b = \left[\frac{6}{L^2}(-1+2\xi), \frac{6}{L^2}(1-2\xi), \frac{2}{L}(2-3\xi), \frac{2}{L}(1-3\xi) \right]$.

The stiffness matrix of the flexural element may then be expressed as

$$\mathbf{K}_i = \int_V \begin{bmatrix} \mathbf{B}_a^T \\ -y\mathbf{B}_b^T \end{bmatrix} E_T [\mathbf{B}_a, -y\mathbf{B}_b] dV = \begin{bmatrix} \int_0^L \mathbf{B}_a^T \mathbf{B}_a \int_A E_T dA dx & \int_0^L \mathbf{B}_a^T \mathbf{B}_b \int_A -y E_T dA dx \\ \int_0^L \mathbf{B}_b^T \mathbf{B}_a \int_A -y E_T dA dx & \int_0^L \mathbf{B}_b^T \mathbf{B}_b \int_A y^2 E_T dA dx \end{bmatrix} \quad (9)$$

where V , A and E_T are the volume, sectional area and the equivalent Young's modulus of the element, respectively.

To evaluate the stiffness matrix, the area integrals representing sectional properties of the elements and integration along the length of the matrix member, as expressed in Eq. (9) must be solved. This study employs a layered approach to solve for the section properties $E_k A_k = \int_A E_T dA$, $E_k S_k = -\int_A E_T y dA$ and $E_k I_k = \int_A E_T y^2 dA$. The advantage of this approach is that the non-linear material variation of the Young's modulus can be easily incorporated into the element stiffness matrix. For steel plate elements, the values of $E_k A_k$, $E_k S_k$ and $E_k I_k$ at $\xi = \xi_k$ may be approximated by the following summation series

$$E_k A_k = \sum_{j=1}^{n_p} E_{pj} A_{pj} \quad (10)$$

$$E_k S_k = -\sum_{j=1}^{n_p} E_{pj} A_{pj} y_{pj} \quad (11)$$

$$E_k I_k = \sum_{j=1}^{n_p} E_{pj} A_{pj} y_{pj}^2 \quad (12)$$

where E_{pj} , A_{pj} and y_{pj} are, respectively, the Young's modulus, the sectional areas and the depth to the centroid of the steel plates evaluated at the j^{th} layer, and n_p is the total layers of the layered model (Fig. 3(a)). Meanwhile, the integration along the length of the element is solved numerically using three-point Gaussian integration. The integration points ξ_k are at $\xi_1 = 0.1127$, $\xi_2 = 0.5$ and $\xi_3 = 0.8873$, and the corresponding weighting factors w_k are $w_1 = 5/9$, $w_2 = 8/9$ and $w_3 = 5/9$. The stiffness matrix of steel plate $\mathbf{K}_{i,p}$ can be obtained using Eq. (9), and the explicit form of the matrix is shown in Appendix A.

For the RC beam elements, the values of $E_k A_k$, $E_k S_k$ and $E_k I_k$ at $\xi = \xi_k$ may be expressed as

$$E_k A_k = \sum_{j=1}^{n_c} E_{c_j} A_{c_j} + \sum_{j=1}^{n_s} E_{s_j} A_{s_j} \quad (13)$$

$$E_k S_k = -\left(\sum_{j=1}^{n_c} E_{c_j} A_{c_j} y_{c_j} + \sum_{j=1}^{n_s} E_{s_j} A_{s_j} y_{s_j} \right) \quad (14)$$

$$E_k I_k = \sum_{j=1}^{n_c} E_{c_j} A_{c_j} y_{c_j}^2 + \sum_{j=1}^{n_s} E_{s_j} A_{s_j} y_{s_j}^2 \quad (15)$$

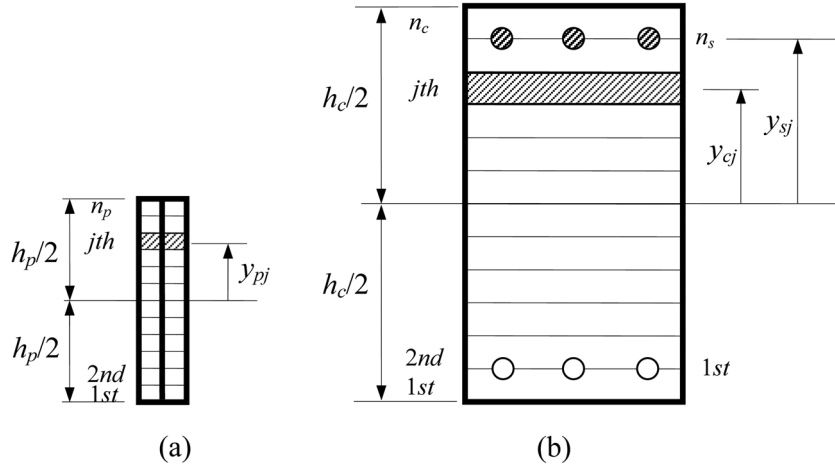


Fig. 3 Layered models of (a) steel plates and (b) reinforced concrete

where E_{cj} , A_{cj} , and y_{cj} are, respectively, the Young's modulus, the sectional areas and the depth to the reference centroidal axis of the concrete; E_{sj} , A_{sj} , and y_{sj} are, respectively, the Young's modulus and the sectional areas of the steel bars, and the depth from the steel bars to the reference centroidal axis of the concrete; and n_c and n_s are the total layers of the layered models for concrete and steel bars (Fig. 3(b)). For the RC beam elements, further transformation is required since the elements are formed by adding two vertical rigid arms of length e (equal to the separation of the centroidal axes of the concrete and steel plates) to the ends of the flexural element (Fig. 2(b)). The transformation matrix for the flexural element connected with two vertical rigid arms of length e is given by

$$\mathbf{T} = \begin{bmatrix} 1 & 0 & -e & 0 & 0 & 0 \\ 0 & 1 & 0 & 0 & 0 & 0 \\ 0 & 0 & 1 & 0 & 0 & 0 \\ 0 & 0 & 0 & 1 & 0 & -e \\ 0 & 0 & 0 & 0 & 1 & 0 \\ 0 & 0 & 0 & 0 & 0 & 1 \end{bmatrix} \quad (16)$$

Multiplying the above transformation matrix with the stiffness matrix as shown in Eq. (9), i.e., $\mathbf{K}_{i,RC} = \mathbf{T}^T \mathbf{K} \mathbf{T}$, the element stiffness matrix for RC beam elements can be obtained. The explicit expression of the matrix is presented in Appendix B.

2.3 Formulation of the stiffness matrix of connecting non-linear bolt groups

The bolt groups connecting the RC beam and the steel plates are subject to combined in-plane moment and shear. As a result, the bolts within the bolt groups deform under a non-linear path. A kinematic hardening model appropriate for simulating the load-deformation response of non-linear bolts under multi-directional shear will be employed in this study. The theory of the model used to simulate a bolt group subjected to a multi-directional shear and deformed along a non-linear path has been previously discussed in detail (Siu and Su 2009). In this section, the formulation of a kinematic hardening model to simulate a bolt under a general shear force will be briefly described.

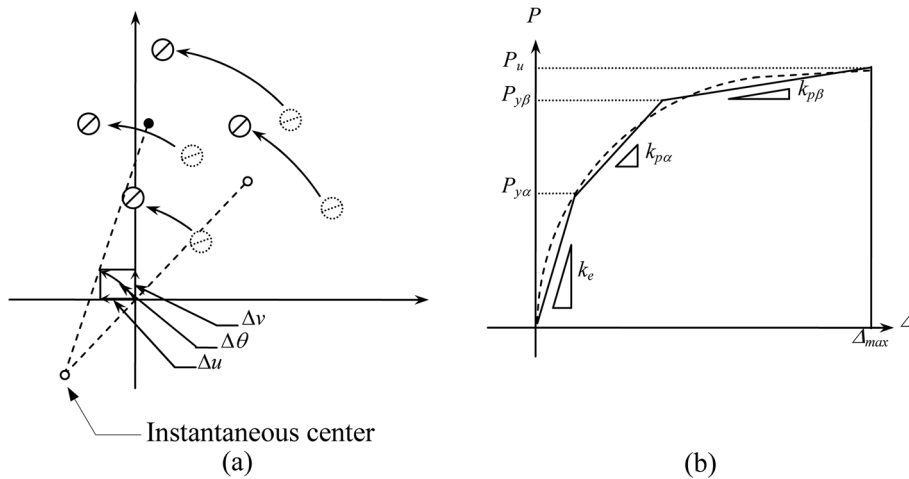


Fig. 4 Assumptions used in bolt group model (a) rigid body movements and (b) idealized tri-linear load-deformation relationship of bolts

Based on the theory, the element stiffness matrix of bolt groups is derived by considering the force equilibrium in the x , y and rotational directions.

The assumptions made within the framework of the formulation are listed as follows:

- 1) Bolts are connected by a plate that acts as rigid (Fig. 4(a)).
- 2) The media which the bolts connect are frictionless.
- 3) The load-deformation relationship of bolts, including the effect of bolt-hole elongation, is assumed to be tri-linear (Fig. 4(b)) and kinematically hardened.
- 4) The bolts are separated widely such that the interference between them can be neglected.
- 5) Failure of individual bolts, and hence the bolt group, is governed by internal bolt forces.

According to the kinematic hardening model of bolts, the current state of a bolt can be defined once the locations of centres of yield surfaces ($\alpha(P_x, P_y)$ and $\beta(P_x, P_y)$) at various loading stages and

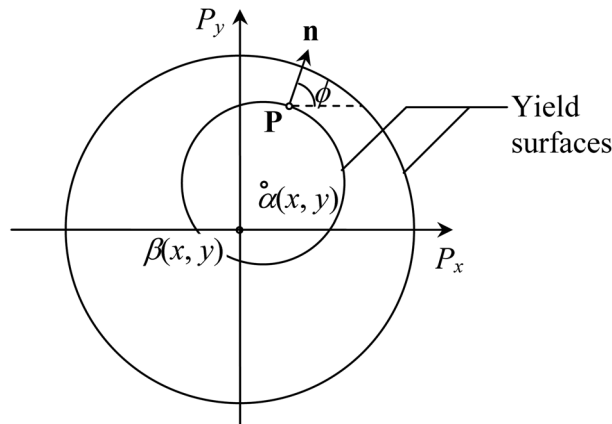


Fig. 5 Parameters for defining the current state of a bolt

the angle ϕ between the x -axis and the direction of normal vectors \mathbf{n} are known. The physical meanings of the associated parameters are illustrated in Fig. 5.

When an incremental load is applied to the bolt, the stiffness of the bolt is k_p in the normal direction and k_e in the tangential direction. The value k_p is equal to one of the stiffness k_e , $k_{p\alpha}$ or $k_{p\beta}$ depending on the current yielding stage. The incremental load-deformation relationship of a bolt can be mathematically expressed as

$$\begin{bmatrix} \Delta P_n \\ \Delta P_t \end{bmatrix} = \begin{bmatrix} k_p & 0 \\ 0 & k_e \end{bmatrix} \begin{bmatrix} \Delta S_n \\ \Delta S_t \end{bmatrix} \quad (17)$$

where the subscripts n and t denote the normal and tangential directions of the yield surface at the loading point, respectively.

By classical bolt group theory, the relationship between the deformation of the i^{th} bolt $(\Delta s_x, \Delta s_y)_i$ and the rigid body movement of the bolt group $(\Delta s_l, \Delta s_v, \Delta s_\theta)$; see also Fig. 4(a)) can be expressed as

$$\begin{bmatrix} \Delta S_x \\ \Delta S_{y_i} \end{bmatrix} = \begin{bmatrix} 1 & 0 & -v_i \\ 0 & 1 & u_i \end{bmatrix} \begin{bmatrix} \Delta s_l \\ \Delta s_v \\ \Delta s_\theta \end{bmatrix} \quad (18)$$

where (u_i, v_i) is the Cartesian coordinate of the bolt.

It has been mentioned in Eq. (17) that once bolt yielding starts, the load-deformation response of the i^{th} bolt can be represented as

$$\begin{bmatrix} \Delta P_n \\ \Delta P_{t_i} \end{bmatrix} = \begin{bmatrix} k_p & 0 \\ 0 & k_e \end{bmatrix} \begin{bmatrix} \Delta s_n \\ \Delta s_{t_i} \end{bmatrix} \quad (19)$$

Applying a coordinate transformation to the global x and y directions, and using Eq. (18), the following relationship can be obtained

$$\begin{bmatrix} \Delta P_x \\ \Delta P_{y_i} \end{bmatrix} = \begin{bmatrix} c & -s \\ s & c \end{bmatrix}_i \begin{bmatrix} k_p & 0 \\ 0 & k_e \end{bmatrix}_i \begin{bmatrix} c & s \\ -s & c \end{bmatrix}_i \begin{bmatrix} 1 & 0 & -v_i \\ 0 & 1 & u_i \end{bmatrix}_i \begin{bmatrix} \Delta s_l \\ \Delta s_v \\ \Delta s_\theta \end{bmatrix}_i \quad (20)$$

Here, c and s correspond to $\cos\phi$ and $\sin\phi$, respectively, with the value of ϕ as indicated in Fig. 5 and equal to $\arg(\hat{\mathbf{n}}_i)$, where $\hat{\mathbf{n}}_i$ is the unitary normal vector on the yield surface at the loading point.

Expanding Eq. (20) and substituting $k = k_e - k_p$, where k represents the stiffness degradation, results in

$$\begin{bmatrix} \Delta P_x \\ \Delta P_{y_i} \end{bmatrix} = \begin{bmatrix} k_e - c^2 k & -c s k & -(k_e - c^2 k)v_i - (c s k)u_i \\ -c s k & k_e - s^2 k & (k_e - s^2 k)u_i + (c s k)v_i \end{bmatrix}_i \begin{bmatrix} \Delta s_l \\ \Delta s_v \\ \Delta s_\theta \end{bmatrix}_i \quad (21)$$

Considering the global force equilibrium of the applied loads and the bolt forces, we have

$$\Delta Q_x = \sum_i \Delta P_{x_i}, \quad \Delta Q_y = \sum_i \Delta P_{y_i} \quad \text{and} \quad \Delta Q_\theta = \sum_i (\Delta Q_{y_i} u_i - \Delta Q_{x_i} v_i) \quad (22)$$

Substituting Eq. (21) into Eq. (22) and rearranging, we have

$$\begin{bmatrix} \Delta Q_x \\ \Delta Q_y \\ \Delta Q_\theta \end{bmatrix} = \begin{bmatrix} K_{cc} & -K_{cs} & -R_{ccy} - R_{csx} \\ -K_{cs} & K_{ss} & R_{ssx} + R_{csy} \\ -R_{ccy} - R_{csx} & R_{ssx} + R_{csy} & I_{ccy} + I_{ssx} + 2I_{cs} \end{bmatrix} \begin{bmatrix} \Delta s_l \\ \Delta s_v \\ \Delta s_\theta \end{bmatrix} \quad (23)$$

where $K_{cc} = \sum_i k_e - c_i^2 k$, $K_{ss} = \sum_i k_e - s_i^2 k$, $K_{cs} = \sum_i c_i s_i k$, $R_{ssx} = \sum_i (k_e - s_i^2 k) x_i$, $R_{ccy} = \sum_i (k_e - c_i^2 k) y_i$,

$R_{csx} = \sum_i c_i s_i x_i k$, $R_{csy} = \sum_i c_i s_i y_i k$, $I_{ccy} = \sum_i (k_e - c_i^2 k) y_i^2$, $I_{ssx} = \sum_i (k_e - s_i^2 k) x_i^2$, and $I_{cs} = \sum_i c_i s_i x_i y_i k$.

Eq. (23) represents the incremental load-deformation relationship of the bolt group under in-plane shear force in any direction and eccentricity at a single load step. In particular, when k equals zero (i.e., all bolts are elastic), all non-diagonal terms become zero, and it represents the elastic case where the behaviour of bolt groups can be simulated by independent springs.

3. Force equilibrium and assemblage of the structural stiffness matrix

The interaction of a general i^{th} bolt groups is illustrated in Fig. 6. By defining a deformation of the bolt group as the movement of steel plates relative to the concrete, the corresponding nodal equilibrium equations for the reinforced concrete and the steel plates are

$$\begin{bmatrix} F_{xb} \\ F_{yb} \\ M_{\theta b} \end{bmatrix}_{i-1}^c + \begin{bmatrix} F_{xa} \\ F_{ya} \\ M_{\theta a} \end{bmatrix}_i^c + \begin{bmatrix} Q_x \\ Q_y \\ Q_\theta \end{bmatrix}_i = 0 \quad (24)$$

$$\begin{bmatrix} F_{xb} \\ F_{yb} \\ M_{\theta b} \end{bmatrix}_{i-1}^p + \begin{bmatrix} F_{xa} \\ F_{ya} \\ M_{\theta a} \end{bmatrix}_i^p - \begin{bmatrix} Q_x \\ Q_y \\ Q_\theta \end{bmatrix}_i = 0 \quad (25)$$

Reinforced concrete beam

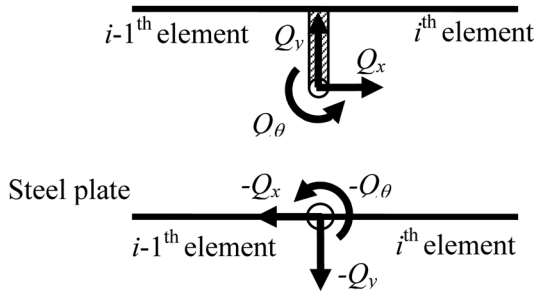


Fig. 6 Force interactions between the bolt group, the steel plate elements and the concrete elements

Considering the load-deformation relationship of the i^{th} bolt group, we have

$$\begin{bmatrix} Q_x \\ Q_y \\ Q_{d_i} \end{bmatrix} = [\mathbf{K}_i]_b \begin{bmatrix} u_i \\ v_i \\ \theta_i \end{bmatrix}^p - \begin{bmatrix} u_i \\ v_i \\ \theta_i \end{bmatrix}^c \quad (26)$$

By defining

$$\begin{aligned} [Q]_i &= [Q_x, Q_y, Q_{d_i}]^T \\ [Q] &= [Q_1^T, Q_2^T, \dots, Q_n^T]^T \\ [d_i]_c &= [u_i, v_i, \theta_i]_c^T \\ [d]_c &= [d_1^T, d_2^T, \dots, d_n^T]_c^T \\ [d_i]_p &= [u_i, v_i, \theta_i]_p^T \\ \text{and } [d]_p &= [d_1^T, d_2^T, \dots, d_n^T]_p^T \end{aligned} \quad (27)$$

and assembling the stiffness matrix equations of all elements in the beam, the equilibrium equation can be represented by

$$[\mathbf{K}]_c [d]_c = [Q] + [F]_c \quad (28)$$

$$[\mathbf{K}]_p [d]_p = -[Q] + [F]_p \quad (29)$$

$$[Q] = [\mathbf{K}]_b [[d]_p - [d]_c] \quad (30)$$

Eliminating the bolt force $[Q]$ in Eq. (28) to Eq. (30), the structural stiffness matrix can be obtained as follows

$$\begin{bmatrix} \mathbf{K}_c + \mathbf{K}_b & \vdots & -\mathbf{K} \\ \vdots & \ddots & \vdots \\ -\mathbf{K}_b & \vdots & \mathbf{K}_p + \mathbf{K}_b \end{bmatrix} \begin{bmatrix} [d]_c \\ [d]_p \end{bmatrix} = \begin{bmatrix} F_c \\ F_p \end{bmatrix} \quad (31)$$

where $[\mathbf{K}]_b = \text{diag}[\mathbf{K}_1, \mathbf{K}_2, \dots, \mathbf{K}_n]_b$, $[F]_c$ and $[F]_p$ are the external load vectors applied to the RC beam and the steel plates.

4. Implementation of the computer program

4.1 Program details

A computer program SiBAN based on the above formulation is developed to simulate the non-linear response of BSP beams. In this program, the stress-strain (σ - ε) relationship adopted for

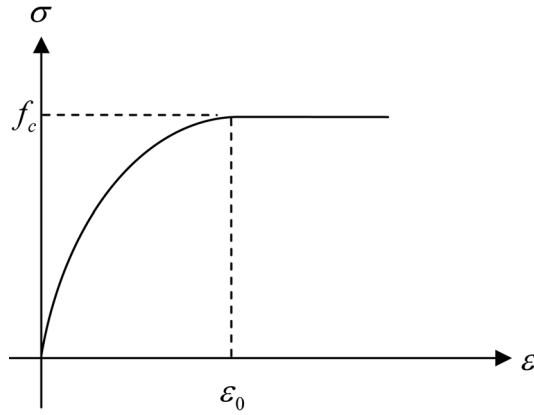


Fig. 7 Stress-strain relationship of concrete adopted by SiBAN

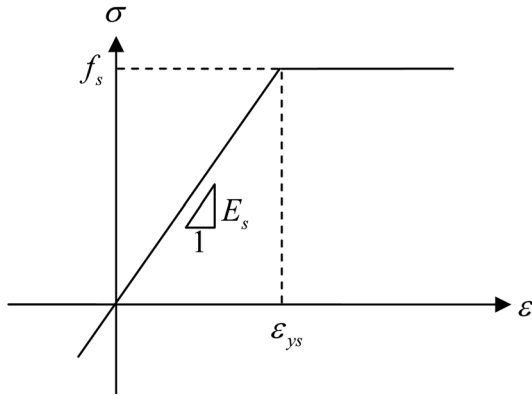


Fig. 8 Stress-strain relationship of reinforcement used by SiBAN

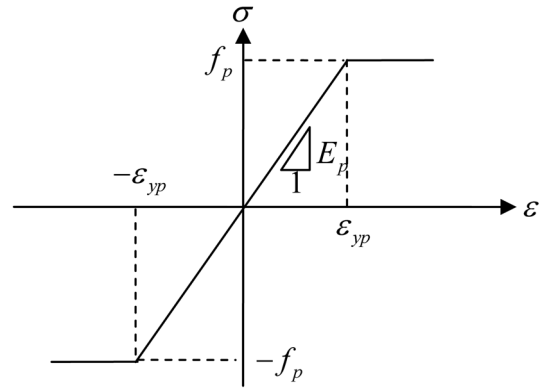


Fig. 9 Stress-strain relationship of steel plates employed in SiBAN

concrete consists of a parabolic relationship up to the peak stress followed by a linear descending relationship in the post-peak region, as illustrated in Fig. 7. It is mathematically expressed as

$$\sigma = f_c \left(2 \frac{\varepsilon}{\varepsilon_0} - \left(\frac{\varepsilon}{\varepsilon_0} \right)^2 \right) \quad \text{for } \varepsilon < \varepsilon_0 \quad (32)$$

$$\sigma = f_c \quad \text{for } \varepsilon \geq \varepsilon_0 \quad (33)$$

where f_c is the uni-axial compressive strength of concrete and ε_0 is chosen as 0.0025 for this simulation.

Elastic-plastic relationships are adopted for both reinforcements and strengthening plates as shown in Figs. 8 and 9 respectively. The mathematical definitions of the stress-strain relationships for steel reinforcement are

$$\sigma = E_s \varepsilon \quad \text{for } -\varepsilon_{ys} < \varepsilon < \varepsilon_{ys} \quad (34)$$

$$\sigma = E_s \varepsilon_{ys} \quad \text{for } \varepsilon \geq \varepsilon_{ys} \quad (35)$$

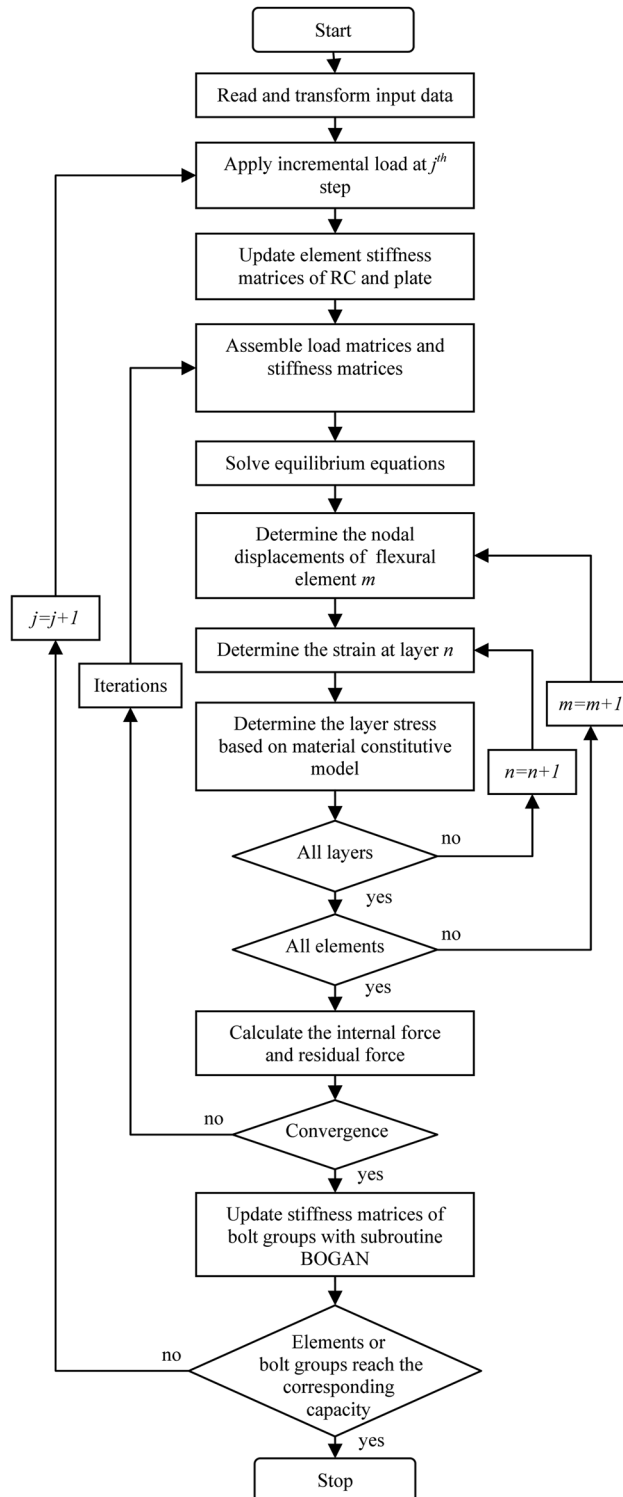


Fig. 10 Solution algorithm used in SiBAN

$$\sigma = -E_s \varepsilon_{y_s} \quad \text{for} \quad \varepsilon \leq -\varepsilon_{y_s} \quad (36)$$

where ε_{y_s} is the yield stress of steel reinforcement. For steel plate, they are

$$\sigma = E_p \varepsilon \quad \text{for} \quad -\varepsilon_{y_p} < \varepsilon < \varepsilon_{y_p} \quad (37)$$

$$\sigma = E_p \varepsilon_{y_p} \quad \text{for} \quad \varepsilon \geq \varepsilon_{y_p} \quad (38)$$

$$\sigma = -E_p \varepsilon_{y_p} \quad \text{for} \quad \varepsilon \leq -\varepsilon_{y_p} \quad (39)$$

where ε_{y_p} is the yield stress of steel plate.

As mentioned in Section 2.3, the load-deformation of anchor bolts under shear is non-linear, with tangential stiffness dropping gradually up to the point of failure. Such a non-linear response was simplified to a tri-linear function for the purposes of simulation. The tri-linear function was governed by the three turning points on the function, as shown in Fig. 4(a). Thus, a total of six parameters ($P_{y\alpha}$, $P_{y\beta}$, P_u , k_e , $k_{p\alpha}$ and $k_{p\beta}$) were required to define the mechanical properties of the anchor bolts.

The detailed procedure of the computer program is shown in Fig. 10 and described below:

Step 1: The required information to specify the program is input.

Step 2: The elastic stiffness matrices of bolt groups are formulated by applying classic theory of bolt groups.

Step 3: An incremental load is applied to drive the load step.

Step 4: The tangential stiffness matrices of the RC and strengthening plates are formulated using the procedure described in Section 2.2 based on the current displacement vector. Together with the stiffness matrices of the bolt groups from the load step, the structural stiffness matrix is assembled.

Step 5: The incremental displacement vector is solved and added to the cumulative displacement vector.

Step 6: The nodal forces are computed using the cumulative displacement vector. The residual force vector is then solved by subtracting the external force vector from the nodal force vector.

Step 7: Convergence checking is performed by examining the error term. If convergence is not satisfied, the residual force vector is input to drive the simulation and Steps 4 to 6 are repeated until convergence is reached.

Step 8: The subroutine BOGAN is carried out by inputting the cumulative displacement vector into the subroutine. At the end of the subroutine, the updated element stiffness matrices of the bolt groups are obtained.

Step 9: The program is proceeds to Step 3, where a further incremental load is applied.

The partial interaction due to the use of bolt groups to transfer shear forces between the RC and steel plates was incorporated into SiBAN using a special subroutine. This subroutine was modified from the computer program BOGAN (Siu and Su 2009), which was developed to compute the load-deformation response of a generally arranged bolt group. In each load step, the solution displacement was input into the subroutine and the yield conditions of bolts and element stiffness matrices for the bolt groups were updated. More details about the solution procedure of the subroutine can be found in previous works by Siu and Su (2009).

An iterative scheme is required to solve the non-linear solution of the BSP beam under loading. In SiBAN, the modified Newton-Raphson method is adopted. This method can reduce the number of

iterations in each load step by updating the structural stiffness matrix in each iteration. The total computational time for the solution procedure can also be reduced.

The error term of iteration is defined as the ratio between root-mean-square (RMS) incremental displacements in the corresponding iteration and the RMS value of the accumulated displacement increment of all iterations in each load step. The convergence criteria are satisfied when the error term is less than 1%. In general, the convergence criteria for the j^{th} iteration of a loading step can be expressed as

$$\sqrt{\frac{\sum_{i=1}^{DOF} (\Delta d_{i,j})^2}{\sum_{i=1}^{DOF} \left(\sum_{k=1}^j \Delta d_{i,k} \right)^2}} \leq 0.01 \quad (40)$$

where $\Delta d_{i,k}$ is the incremental displacement of the i^{th} DOF in the k^{th} iteration.

5. Experimental verification

5.1 General description of the experiment

A series of BSP beam tests aimed at investigating the flexural behaviour of BSP beams with partial interaction was carried out (Siu and Su 2010). The experimental programme consisted of four BSP beams with the same RC geometry but different bolt-plate arrangements (see Fig. 11). 3T16 reinforcement was adopted as the tension reinforcement and 2T10 reinforcement was used as hangers. T10-150 stirrups were installed along the span of the beam so that all strengthened beams were controlled by bending. Mild steel plates with two types of dimensions were used to strengthen the RC beams. The material properties of the concrete, steel reinforcement and steel plates are summarized in Tables 1 and 2. Properly selected bolt group arrangements were used in the four specimens, so that a full range of partial interactions was covered in the study. The beams were simply-supported with a clear span of 3600 mm and loaded symmetrically in four-point bending with point loads 600 mm from either side of the mid-span, as illustrated in Fig. 12.

Anchor bolts with $\phi 12$ HAS-E rods (Hilti Corporation 2005) were used to anchor steel plates to the side faces of the beams. In practical cases, slips due to clearance holes usually occur and would affect the load-deformation response of bolts. In order to minimize this undesirable and random effect, the bolt holes in the concrete and the clearance holes in the steel plates and anchor rods were filled with RE-500, an epoxy provided by HILTI Corporation. Dynamic sets were used to facilitate the injection process and ensure that all gaps were sealed. The detail arrangement of dynamic set with the anchor rods is illustrated in Fig. 13. This arrangement ensured that the uneven distribution of loads on bolts due to random bolt slips would be eliminated and the partial interaction was solely due to the deformations of bolts and the adjacent steel or concrete components.

The bolts were tightened with negligible torque with a spanner so that the friction between the RC beam and steel plates is negligible. A simple bolt shear test setup, as illustrated in Fig. 14, was designed to measure the load-deformation relationship of the anchor bolts under shear. Two bolt specimens were tested. The results showed that a bi-linear relationship (as shown in Fig. 15) is good

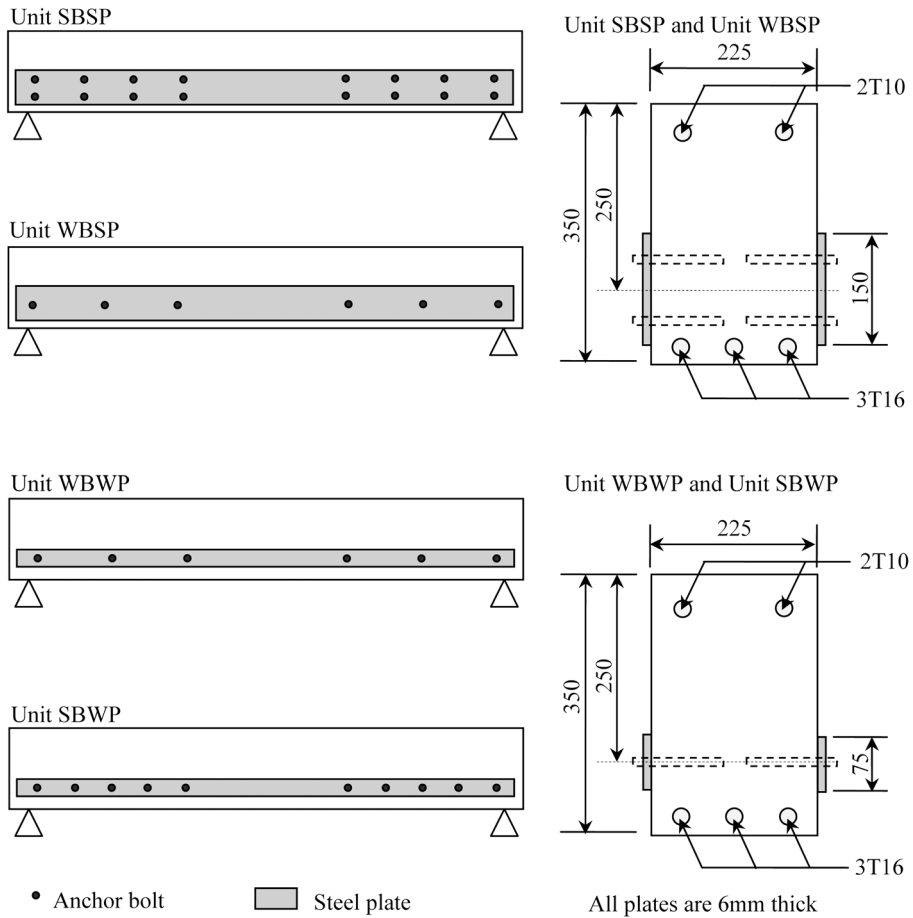


Fig. 11 Detailed arrangements of strengthened specimens

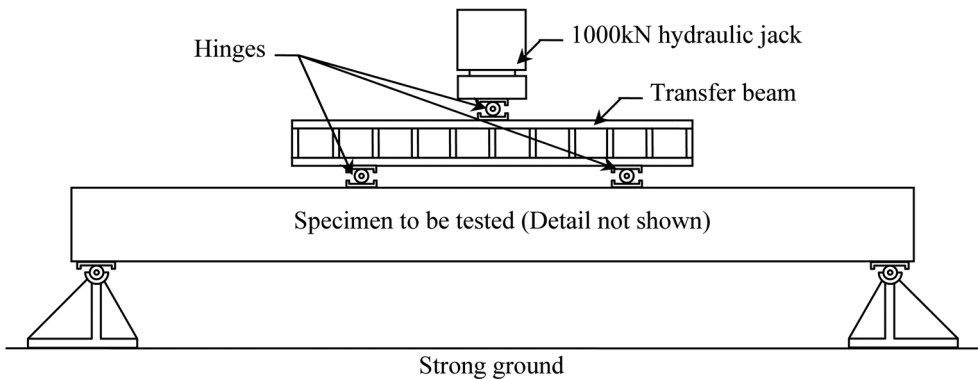


Fig. 12 Experimental Setup

enough to represent the load-deformation relationship of a bolt. Hence, a bi-linear relationship was adopted instead of a tri-linear one to model the load-deformation relationship of a bolt.

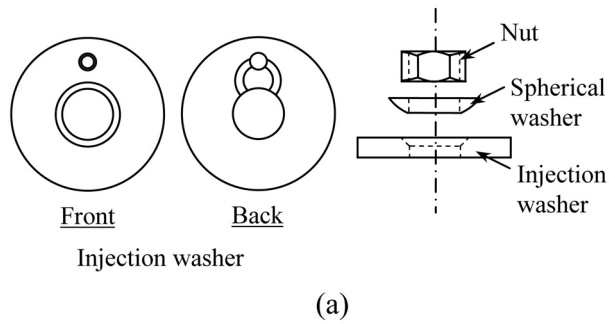


Fig. 13 Dynamic set washer (a) diagrammatic illustration and (b) actual arrangement

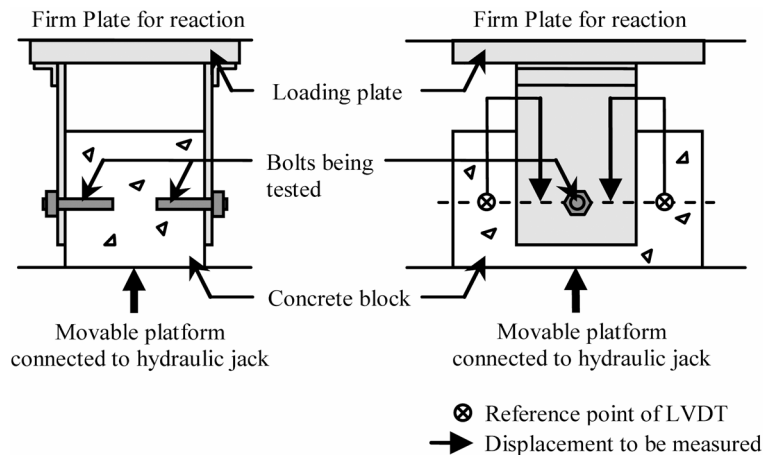
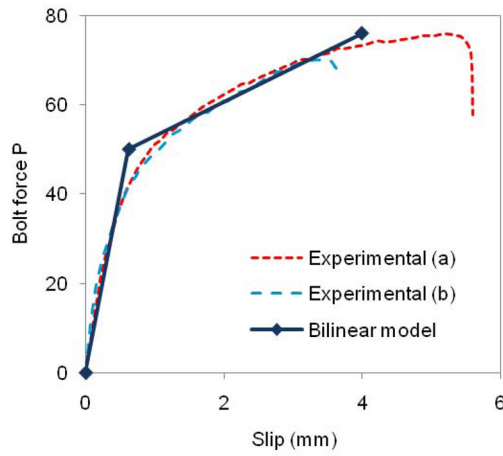


Fig. 14 Bolt shear test setup

5.2 Verification of the computer program

Structural responses of the strengthened specimens were simulated using SiBAN. The load-deflection relationships at mid-span and the longitudinal slip responses were calculated and compared with the experimental results (Siu and Su 2010) to validate the proposed theory and the computer program.

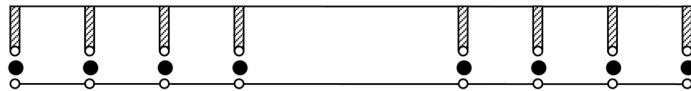
The structural models for all specimens are shown in Fig. 16. Entire specimens were divided into



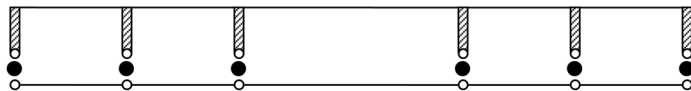
	Slip (mm)	Bolt force (kN)
P ₁	0.625	50
P ₂	4.0	76

Fig. 15 Bi-linear load-deformation model of anchor bolts

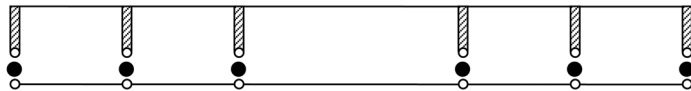
Unit SBSP



Unit WBSP



Unit WBWP



Unit SBWP

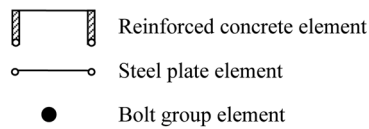


Fig. 16 Finite element models used in the computer program SiBAN

Table 1 Summary of the material properties of specimens

Concrete	Reinforcement		Steel plate	
f_{cu} (MPa)	E_s (GPa)	f_{ys} (MPa)	E_p (GPa)	f_{yp} (MPa)
35	187	537	208	337

Table 2 Concrete mix adopted in the experimental study

	Water	Cement	Fine aggregate	10 mm aggregate
kg/m ³	199.6	278.9	1024.5	837.6

Table 3 Comparison of peak loads obtained from the present numerical analysis and previous experiments

Unit	Peak loads (kNm)		% error
	Test results (Siu and Su 2010)	Present analysis	
SBSP	162	160	-1.2
WBSP	149	146	-2.0
WBWP	133	132	-0.8
SBWP	145	134	-7.6

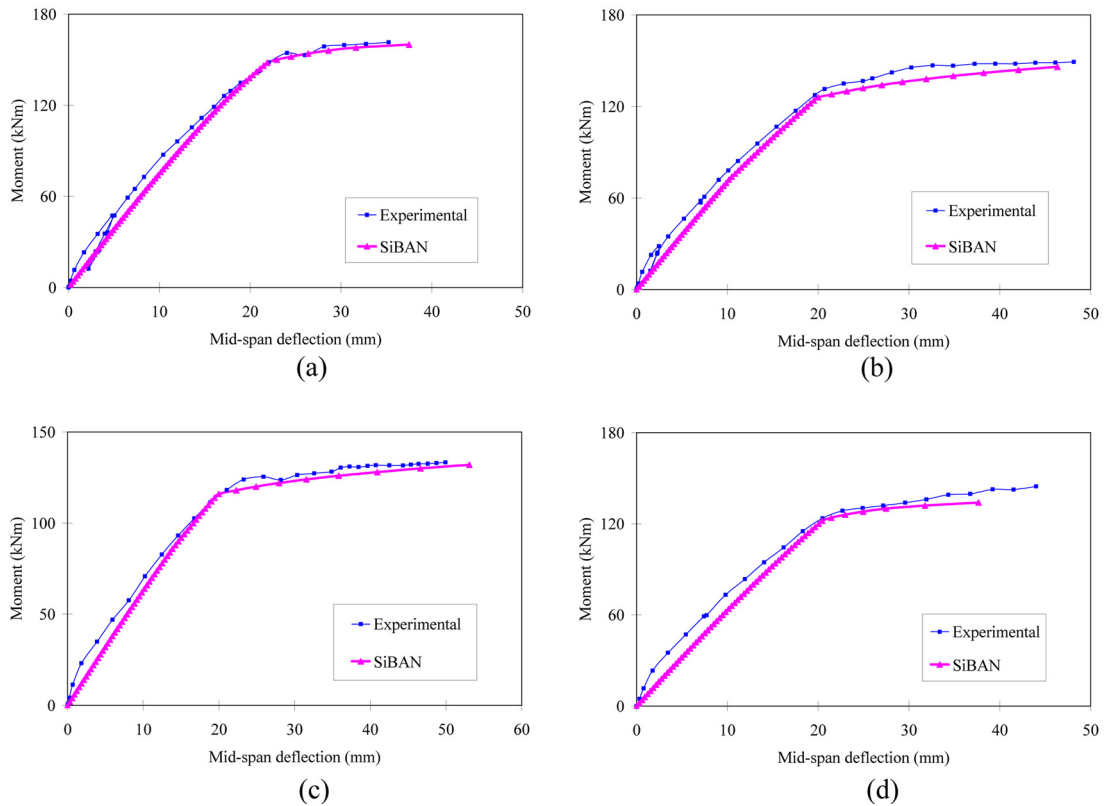


Fig. 17 Comparison of mid-span load-deformation responses of (a) Unit SBSP, (b) Unit WBSP, (c) Unit WBWP and (d) Unit SBWP

five to nine macro-finite-elements depending on the number of bolt groups used in the specimens. The centroidal axes for the RC in all simulations were set at the mid-depth, i.e., the separation of the centroidal axes of RC and steel plates was 75 mm.

The material properties of concrete, reinforcements, steel plates and anchor bolts required in the numerical simulations are listed in Table 1 and shown in Fig. 15.

The peak moments of specimens predicted by SiBAN are listed and compared with the experimental results in Table 3. The numerical simulation provided close estimations of peak moment responses with errors ranging from 0.8% to 7.6%, showing that the effect of partial interactions is properly considered in the present analysis.

The mid-span moment-deflection curves of specimens computed by SiBAN together with the experimental results are plotted in Fig. 17. As there was no node at the mid-span of the structural models, the mid-span deflections were obtained by displacement interpolation. Substituting $\zeta = 0.5$ into Eq. (2), the mid-span deflection can be expressed in terms of the corresponding element nodal displacement vector as

$$v_{c,mid} = \left[\frac{v_a + v_b}{2} + \frac{L(\theta_a - \theta_b)}{8} \right] \quad (40)$$

Fig. 17 shows that the numerical results are consistent with the experimental results up to the peak loads. The initial stiffness of the experimental results is slightly higher than the numerical results. This is because the stiffness contributions from concrete in tension were ignored in the

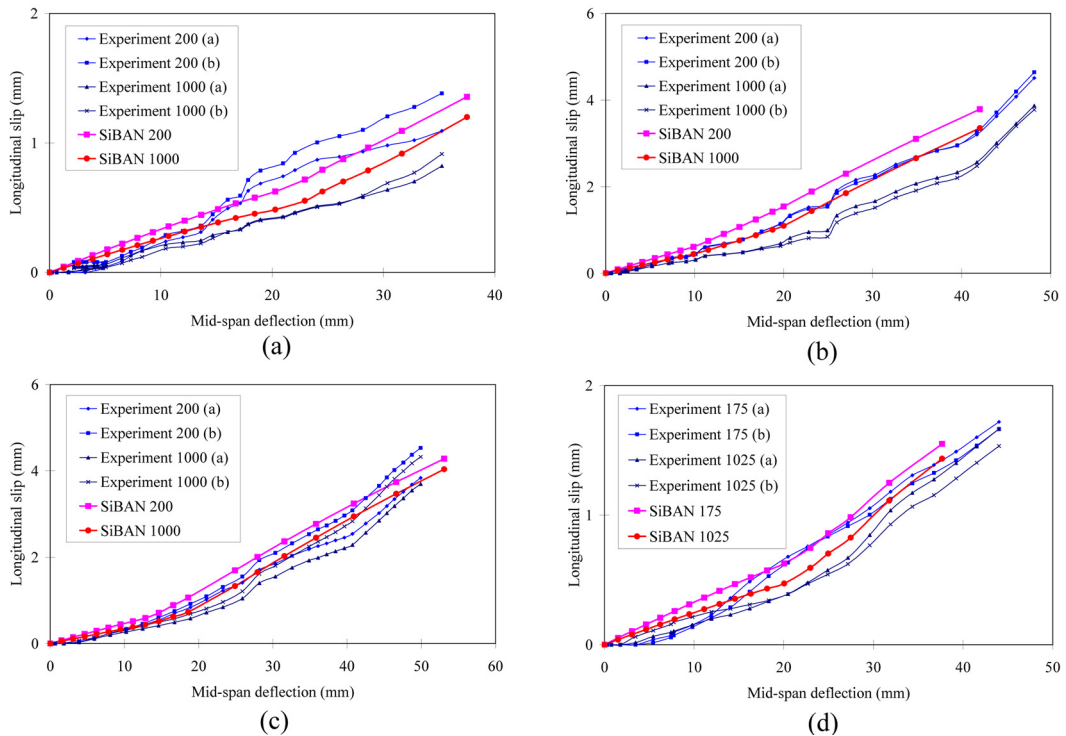


Fig. 18 A comparison of longitudinal slip responses of (a) Unit SBSP, (b) Unit WBSP, (c) Unit WBWP and (d) Unit SBWP

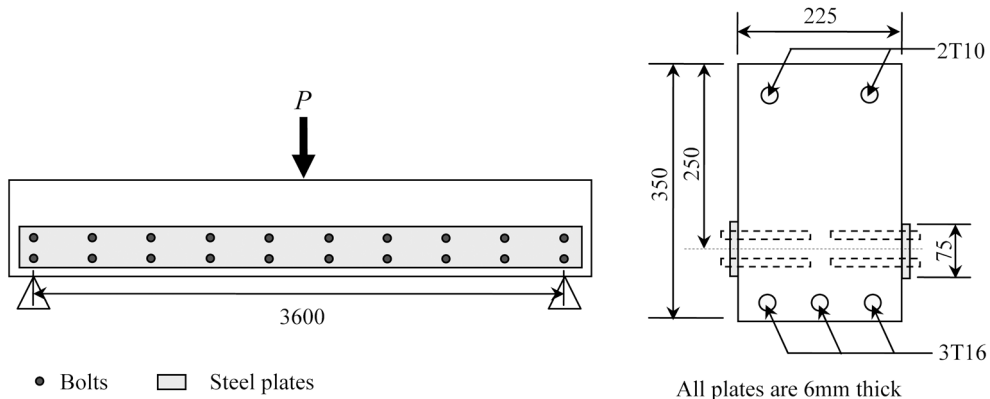


Fig. 19 A beam model for the investigation of bolt-slips

numerical simulation. The experimental and numerical results agree closely with each other as further loads were applied. The turning point in the ascending branch of the curves corresponds to the stage where the tension reinforcement began to yield, which was successfully predicted by the numerical simulations.

As the objective of the current study is to investigate the pre-peak responses of the BSP beams and the program was developed based on a load-controlled solution procedure, it is not currently able to simulate the post-peak response of beams.

The longitudinal slip response of specimens at different sections was extracted by linear interpolation using nodal slip response and plotted in Fig. 18. The numerical results computed by SiBAN generally agree well with the experimental results. We observed that the numerical slip estimated by SiBAN is slightly higher than in the experimental results when initial loading is applied. This is due to the fact that the frictional resistance between the surfaces was ignored when adopting a bi-linear approximation for the uni-directional load-deformation relationship of bolts. The frictional resistance increases the initial stiffness of bolts, which reduces the longitudinal slip responses of the specimens.

From the above comparisons, it can be seen that SiBAN is capable of modelling the overall responses of BSP beams with accurate consideration for partial interactions. In the following section, SiBAN will be used to determine the complete bolt slip response along the span of BSP beams.

6. Slip responses of BSP beams

6.1 Numerical model

Slip responses in the longitudinal and transverse directions have been addressed and described by previous researchers (Oehlers *et al.* 1997). However, comprehensive and quantitative studies have yet to be done to illustrate the actual slip responses along the span of BSP beams, especially in the inelastic stage when a plastic hinge is formed in the RC components. Hence, numerical simulations were carried out using SiBAN to investigate the slip responses of BSP beams. Besides longitudinal and transverse slips, the rotational slip (where the RC and plate rotate relative to each other) was

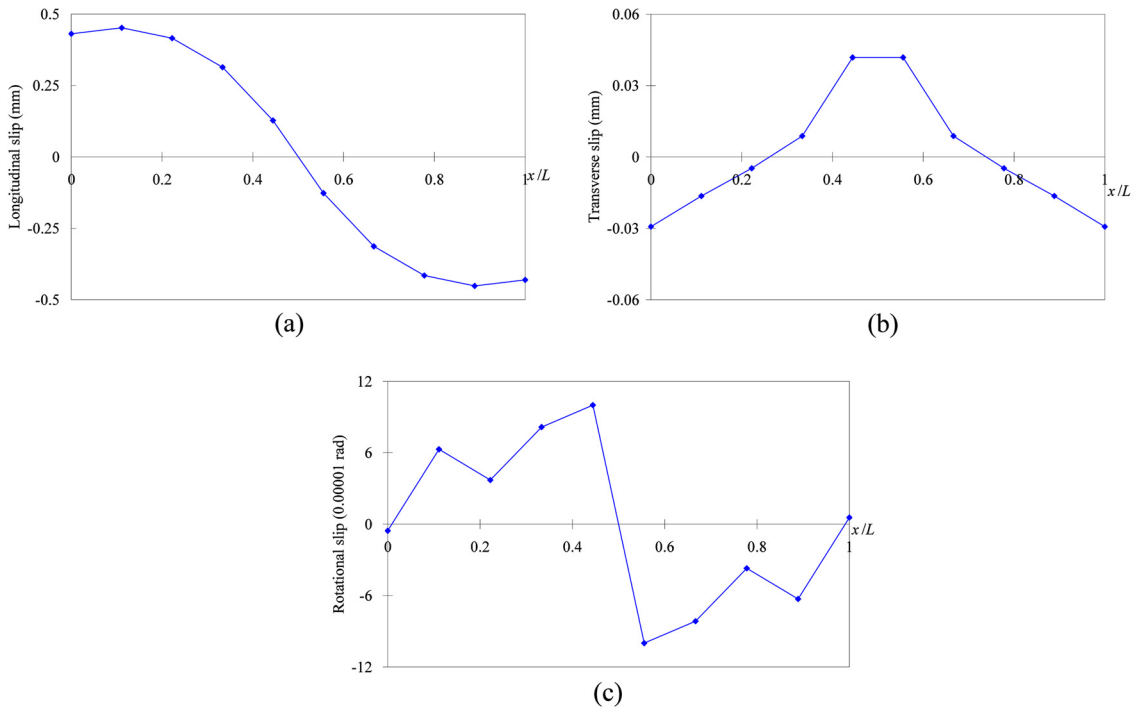


Fig. 20 Slip responses in the elastic stage (i.e., at 50% of the peak load) (a) longitudinal slip profile, (b) transverse slip profile and (c) rotational slip profile

also identified. Variations in slips along the beams were studied in detail.

The beam considered here has the same RC section as that of the specimen adopted in the previous experimental study. The strengthened plate arrangement is the same as Specimen SBSP, while uniform bolt arrangements are adopted across the entire span of the beam (Fig. 19). The beam was loaded with an incremental mid-point load. As there is no node at the mid-span, the mid-point load was transformed into the equivalent load vectors and applied at the corresponding nodes.

Simulations were carried out and the bolt slips along the beam span at 50% and 100% of the peak load were extracted to illustrate the non-linear slip responses of partially interacted BSP beams in the elastic and inelastic stages. The corresponding variations are presented in Figs. 20 and 21.

6.2 Longitudinal and transverse slips

The longitudinal slip profile along the span of the beam in the elastic stage is shown in Fig. 20(a). The slip profile is continuous and anti-symmetric about the mid-span of the beam. The slip is zero at the mid-span and increases gradually with a decreasing rate to reach a maximum at a position close to, but not exactly at, the end supports (at the 1st interior bolt group in this example). While the occurrence of maximum longitudinal slip is not at the end span, the longitudinal slip is almost constant near the end supports. For simplicity, we may assume that the position of the maximum longitudinal slips occurred at the supported ends.

As the beam approached the inelastic stage (Fig. 21(a)), the slip strain (i.e., the 1st derivative of

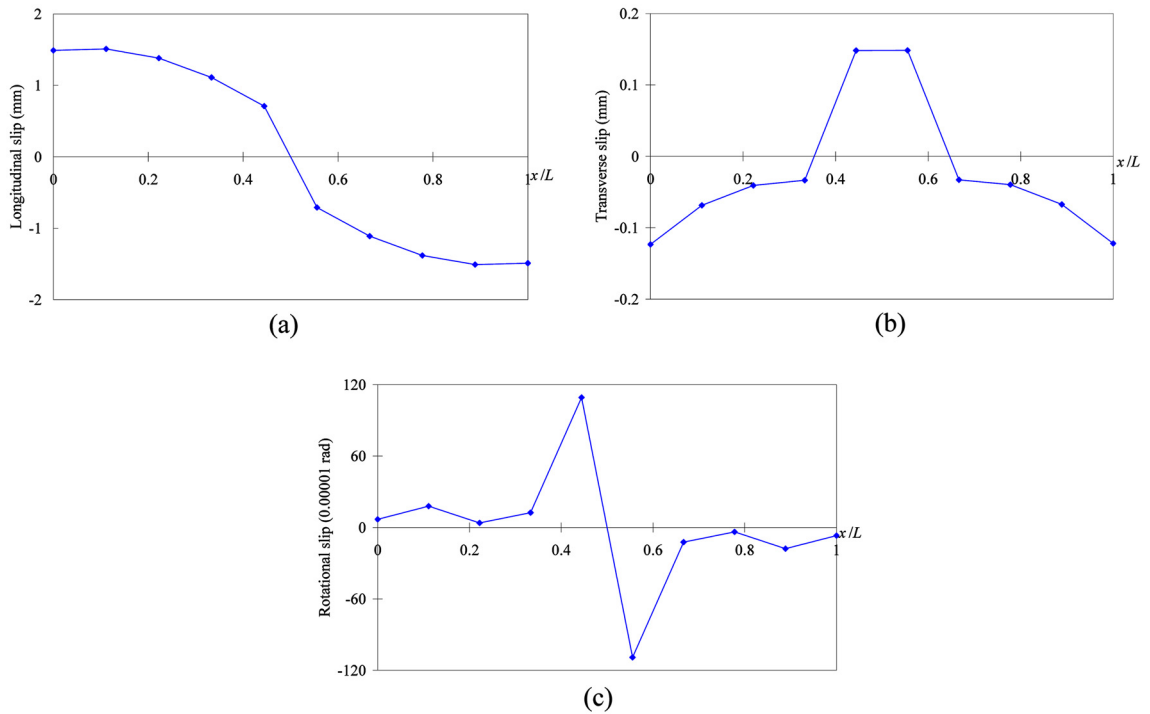


Fig. 21 Slip responses in the inelastic stage (i.e., at the peak load) (a) longitudinal slip profile, (b) transverse slip profile and (c) rotational slip profile

slip about x) increased faster at the mid-span and corresponded to a change in the slip profile. This change was mainly due to the gradual formation of a plastic hinge at the mid-span. When the plastic hinge gradually formed, the flexural stiffness of the section dropped, causing the strain of the concrete at the centroidal axis of plate (ε_{c,h_p}) to increase more quickly. As the slip strain is equal to $\varepsilon_{p,h_p} - \varepsilon_{c,h_p}$, the slip strain would also increase faster accordingly. Such a higher rate of increase in slip strain at the mid-span (or at the location of critical sections) reduces the partial interaction between the RC and steel plate, which further reduces the ultimate strength of the member. Hence, the non-linear effect due to the occurrence of the plastic hinge should be considered in the analysis of bolted sided-plated RC beams.

The transverse slip profiles along the span in both the elastic and inelastic stages (Figs. 20(b) and 21(b), respectively) were quite similar. Being symmetric about the mid-span, the transverse slip is positive at regions near the mid-span and negative at regions near the two supports. In other words, the steel plate moves upward relative to the RC beam at the mid-span and downward near the supports. The total bolt slips in the positive zone and negative zones are equal in the elastic stage so that the vertical force equilibrium of the steel plates is maintained.

Further considering the relative magnitude between the longitudinal and transverse slips, it can be seen that the maximum longitudinal slip along the span is about ten times the maximum transverse slip in both the elastic and inelastic stage. This was consistent with the findings of Oehlers *et al.* (1997), who reported that the slip response of bolts is dominant in the longitudinal direction.

6.3 Rotational slips

While the influence of translational partial interaction in the x - (longitudinal) and y - (transverse) directions has been well studied by previous researchers, the effect of rotational partial interaction between RC and steel plates has not been investigated. The rotational slip is the relative rotation between the cross sections of the RC and the steel plates, and will occur simultaneously with the presence transverse partial interaction.

When the transverse partial interaction is present, due to the vertical force equilibrium, the transverse slip varies from negative at supports to positive values at the mid-span, as described in the previous section. This implies that the first derivative of the transverse slip with respect to x is non-zero. This non-zero derivative is equal to the rotational slip in mathematical terms, since the rotation of a member is equal to the first derivative of the vertical displacement.

The rotational slip affects the slip responses of bolts when more than one row of bolts is installed, or the bolts are not installed along the centroidal axis of the plate. Excess rotation between the two media will result in an uneven distribution of bolt forces on the same transverse plane.

The variation of rotational slip is anti-symmetric about the mid-span. In the elastic stage, the rotational slip at the supports is almost zero, while the rotational slips for each of the shear spans are of the same sign. The peak rotational slips occur near the mid-span of the beam, and drop rapidly to zero at the mid-span, as shown in Fig. 20(c).

Figs. 20(c) and 21(c) show the inelastic rotational slips near the mid-span as they increase to ten times the elastic value at the ultimate stage, but only about three times for the other parts of the beam. The results indicate that the rotational slip concentrates at the regions close to the plastic hinges in the ultimate state, adding significant slip demand to the corresponding bolts. Special consideration should be made for the effects of rotational slip concentrations when future studies are conducted.

7. Conclusions

In this paper, a nonlinear analysis for BSP beams was developed. The analysis can accurately predict the load-deformation response and the slips between components, and was developed based on a finite element method. A layered approach was used in order to account for the material nonlinearity of RC. Partial interactions between the RC beam and the strengthening plates were modelled by considering the RC beam and strengthening plates as separate elements interacting through bolt groups.

The nonlinear load-deformation relationship of bolt groups and a tangential element stiffness matrix were developed and incorporated into the macro-finite-element method. A kinematic hardening assumption was made for the connecting bolts and the tangential stiffness matrix of the bolt group was derived using a further application of the bolt group theory,

The overall theory was implemented in a computer program validated by experimental results. Using the validated program, numerical examples were given to illustrate partial interactions in BSP beams. It was observed that the slip response is dominant in the longitudinal direction. The effect of material non-linearity on the slip response should be properly considered in the partial interaction analysis in order to determine the ultimate capacity of BSP beams. The concept of rotational slip was introduced. Rotational slip may cause additional and significant slip demands on a beam.

Further studies to investigate the effects of rotational slip on the structural response of BSP beams are suggested.

Acknowledgements

The research described here was supported by the Research Grants Council of Hong Kong SAR (Project No. HKU7166/08E). Anchor bolts were generously supplied by HILTI Corporation and are gratefully acknowledged.

References

- Ahmed, M., Oehlers, D.J. and Bradford, M.A. (2000), "Retrofitting reinforced concrete beams by bolting steel plates to their sides. Part 1: Behaviour and experimental work", *Struct. Eng. Mech.*, **10**(3), 211-226.
- Arizumi, Y. and Hamada, S. (1981), "Elastic-plastic analysis of composite beams with incomplete interaction by finite element method", *Comput. Struct.*, **14**, 453-362.
- Ayoub, A. (2000), "Mixed formulation of nonlinear steel-concrete composite beam element", *J. Struct. Eng. - ASCE*, **126**(3), 371-381.
- Dall'Asta, A. and Zona, A. (2004), "Three-field mixed formulation for the non-linear analysis of composite beams with deformable shear connection", *Finite Elem. Anal. Des.*, **40**, 425-448.
- Daniels, B.J. and Crisinel, M. (1993), "Composite slab behavior and strength analysis. Part 1: Calculation procedure", *J. Struct. Eng. - ASCE*, **119**(1), 16-35.
- Faella, C., Martinelli, E. and Nigro, E. (2002), "Steel and concrete composite beams with flexible shear connection: "exact" analytical expression of the stiffness matrix and applications", *Comput. Struct.*, **80**, 1001-1009.
- Gattesco, N. (1999), "Analytical modeling of nonlinear behavior of composite beams with deformable connection", *J. Constr. Steel Res.*, **52**, 195-218.
- Hilti Corporation (2005), *Fastening technology manual*, Issue 2005-06.
- Johnson, R.P. and Molenstra, N. (1991), "Partial shear connection in composite beams in buildings", *Proc. Inst. Civil Eng.*, **91**, 679-704.
- Oehlers, D.J., Nguyen, N.T., Ahmed, M., and Bradford, M.A. (1997), "Transverse and longitudinal partial interaction in composite bolted side-plated reinforce-concrete beams", *Struct. Eng. Mech.*, **5**(5), 553-564.
- Oehlers, D.J., Ahmed, M., Bradford, M.A. and Nguyen, N.T. (2000), "Retrofitting reinforced concrete beams by bolting steel plates to their sides. Part 2: Transverse interaction and rigid plastic design", *Struct. Eng. Mech.*, **10**(3), 227-243.
- Ranzi, G., Bradford, M.A. and Uy, B. (2004), "A direct stiffness analysis of a composite beam with partial interaction", *Int. J. Numer. Meth. Eng.*, **61**, 657-672.
- Siu, W.H. and Su, R.K.L. (2009), "Load-deformation prediction of bolt group by a kinematic hardening approach", *J. Constr. Steel Res.*, **65**(2), 436-442.
- Siu, W.H. and Su, R.K.L. (2010), "Effects of plastic hinges on partial interaction behaviour of bolted side-plated beams", *J. Constr. Steel Res.*, **66**(5), 622-633.
- Yam, L.C.P. and Chapman, J.C. (1968), "The inelastic behaviour of simply supported composite beams of steel and concrete", *Proc. Inst. Civil Eng.*, **41**(1), 651-683.

Appendix A

The explicit form of a flexural steel plate element

$$\mathbf{K}_{i,p} = \begin{bmatrix} c_1 & c_8 & c_9 & -c_1 & -c_8 & c_{10} \\ & c_2 & c_3 & -c_8 & -c_2 & c_7 \\ & & c_4 & -c_9 & -c_3 & c_6 \\ & & & c_1 & c_8 & -c_{10} \\ sym. & & & & c_2 & -c_7 \\ & & & & & c_5 \end{bmatrix} \quad (A1)$$

where

$$c_1 = \frac{1}{2L} \sum_{k=1}^3 E_k A_k w_k$$

$$c_2 = \frac{18}{L^3} \sum_{k=1}^3 E_k I_k (2p_k - 1)^2 w_k$$

$$c_3 = \frac{6}{L^2} \sum_{k=1}^3 E_k I_k (2p_k - 1)(3p_k - 2) w_k$$

$$c_4 = \frac{2}{L} \sum_{k=1}^3 E_k I_k (3p_k - 2)^2 w_k$$

$$c_5 = \frac{2}{L} \sum_{k=1}^3 E_k I_k (3p_k - 1)^2 w_k$$

$$c_6 = \frac{6}{L} \sum_{k=1}^3 E_k I_k (3p_k - 1)(3p_k - 2) w_k$$

$$c_7 = \frac{6}{L^2} \sum_{k=1}^3 E_k I_k (3p_k - 1)(2p_k - 1) w_k$$

$$c_8 = \frac{3}{L^2} \sum_{k=1}^3 E_k S_k (1 - 2p_k) w_k$$

$$c_9 = \frac{1}{L} \sum_{k=1}^3 E_k S_k (2 - 3p_k) w_k$$

$$c_{10} = \frac{1}{L} \sum_{k=1}^3 E_k S_k (1 - 3p_k) w_k$$

Appendix B

The explicit form of a flexural RC element

$$\mathbf{K}_{i,RC} = \begin{bmatrix} a_1 & a_8 & a_9 & -a_1 & -a_8 & a_{10} \\ & a_2 & a_3 & -a_8 & -a_2 & a_7 \\ & & a_4 & -a_9 & -a_3 & a_6 \\ & & & a_1 & a_8 & -a_{10} \\ sym. & & & & a_2 & -a_7 \\ & & & & & a_5 \end{bmatrix} \quad (\text{B1})$$

where

$$a_1 = \frac{1}{2L} \sum_{k=1}^3 E_k A_k w_k$$

$$a_2 = \frac{18}{L^3} \sum_{k=1}^3 E_k I_k (2p_k - 1)^2 w_k$$

$$a_3 = \frac{6}{L^2} \sum_{k=1}^3 E_k I_k (2p_k - 1)(3p_k - 2) w_k - \frac{3e}{L^2} \sum_{k=1}^3 E_k S_k (1 - 2p_k) w_k$$

$$a_4 = \frac{2}{L} \sum_{k=1}^3 E_k I_k (3p_k - 2)^2 w_k - \frac{2e}{L} \sum_{k=1}^3 E_k S_k (2 - 3p_k) w_k + \frac{e^2}{2L} \sum_{k=1}^3 E_k A_k w_k$$

$$a_5 = \frac{2}{L} \sum_{k=1}^3 E_k I_k (3p_k - 1)^2 w_k + \frac{2e}{L} \sum_{k=1}^3 E_k S_k (1 - 3p_k) w_k + \frac{e^2}{2L} \sum_{k=1}^3 E_k A_k w_k$$

$$a_6 = \frac{6}{L} \sum_{k=1}^3 E_k I_k (3p_k - 1)(3p_k - 2) w_k - \frac{e}{L} \sum_{k=1}^3 E_k S_k (3 - 6p_k) w_k + \frac{e^2}{2L} \sum_{k=1}^3 E_k A_k w_k$$

$$a_7 = \frac{6}{L^2} \sum_{k=1}^3 E_k I_k (3p_k - 1)(2p_k - 1) w_k + \frac{3e}{L^2} \sum_{k=1}^3 E_k S_k (1 - 2p_k) w_k$$

$$a_8 = \frac{3}{L^2} \sum_{k=1}^3 E_k S_k (1 - 2p_k) w_k$$

$$a_9 = \frac{1}{L} \sum_{k=1}^3 E_k S_k (2 - 3p_k) w_k - \frac{e}{2L} \sum_{k=1}^3 E_k A_k w_k$$

$$a_{10} = \frac{1}{L} \sum_{k=1}^3 E_k S_k (1 - 3p_k) w_k + \frac{e}{2L} \sum_{k=1}^3 E_k A_k w_k$$